Chapter 1

Introduction

1.1 Quantum networks

Quantum networks open a broad frontier of scientific opportunities in quantum information science, including for quantum computation, communication, metrology, and simulation[1]. For example, a quantum network can serve as a 'web' for connecting quantum processors for computation[2,3] and communication[4], as well as a 'simulator' for enabling investigations of quantum critical phenomena arising from interactions among the nodes mediated by the channels[5,6].

Apart from any algorithmic benefit, an important characteristics of a quantum network is shown by comparing the complexity of a problem to describe a quantum network, comprised of N quantum nodes (each with n qubit registers) with fully quantum connectivity, to that of a network of quantum nodes which only share classical channels (see, e.g., refs.[1,7]). The classical information required to represent a density matrix $\hat{\rho}_{\mathrm{QN}}$ of a fully quantum network is $I_{\mathrm{QN}} = 2^D = 4^{N\times n}$, where the dimensionality is $D = 2^{N\times n}$. In contrast, the size of the density matrix $\hat{\rho}_{\mathrm{N}}$ for a network that has only classical connectivity is given by $I_{\mathrm{N}} = N \times 4^n$.

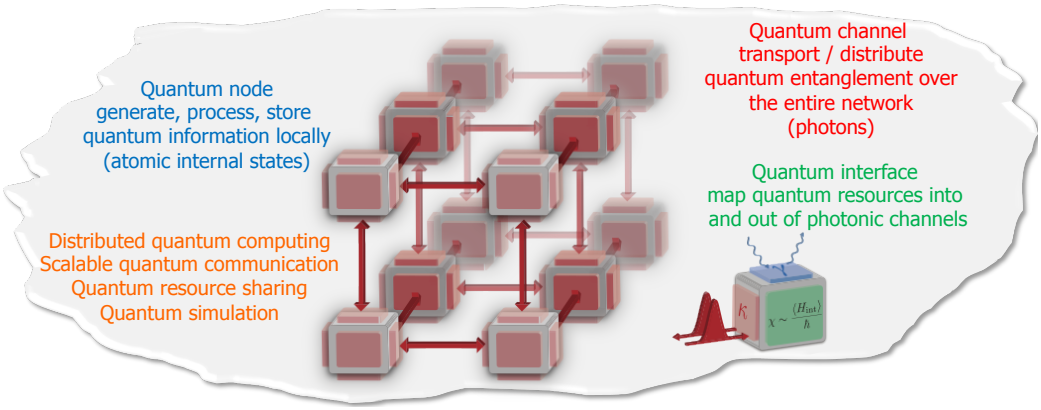

Figure 1.1: **A generic form of a quantum network composed of many quantum nodes and channels[1].** The quantum nodes (box) interact coherently each other by transporting and distributing entanglement over quantum channels (arrows). An important component for these quantum interconnects is a quantum interface for mapping the quantum resources generated from the quantum nodes into and out of the photonic channels.

Therefore, even for moderate parameters $\{N, n\} = \{10, 14\}$ for the fully quantum network, the number of classical variables $I_{\text{QN}} = 4^{140} \sim \mathcal{O}(10^{84})$ to describe $\hat{\rho}_{\text{QN}}$ can greatly exceed the number of hydrogen atoms $\mathcal{O}(10^{80})$ in the observable universe, whereas its classical counterpart $\hat{\rho}_{\text{N}}$ only yields $I_{\text{N}} = 10 \times 4^{14} \sim \mathcal{O}(10^{9})$.

While this complexity also points to the difficulty of controlling and characterizing a large-scale quantum system as $\hat{\rho}_{\text{QN}}$, quantum networks can harness physical processes to benefit from the intricacies introduced by these multipartite quantum states for quantum information processing [1–9], with rudimentary capability of the network enabled by the coherent control of quantum and entangled states of matter and light [1]. Indeed, theoretical inventions of quantum error correction and fault-tolerant quantum computing [10–16], entanglement purification and distillation [17–19], as well as privacy amplification and information reconciliation [20–23] have enabled the promising prospects for experimental implementations of distributed quantum computation [7,24], quantum resource sharing [25,26], scalable quantum communication [4,9], and quantum simulations [5,6] by way of quantum networks.

As illustrated in Fig. 1.1, the physical realization of quantum networks composed of many quantum nodes and channels [1,8,9] requires quantum dynamical systems capable of generating and storing entangled states among multiple quantum memories, and of efficiently transferring stored entanglement into quantum channels [27–33]. Such an interconnect can be achieved by utilizing the strong interactions of single photons and collective excitations in atomic ensembles for the coherent control of entanglement between matter and light [27,30,33], thereby enabling the distribution and teleportation of quantum states across the quantum network [4]. Thus, my thesis will focus on addressing specific challenges to achieve quantum networks: (1) by developing novel laboratory capabilities to generate, store, and control entangled states of matter and light [30,33–35], (2) by implementing various quantum information protocols [36,37], and (3) by devising efficient theoretical tools for multipartite entanglement characterization [33,35,38].

In a broader scope, the research for attaining quantum control over macroscopic quantum coherence and statistics represents an area of fundamental importance beyond of quantum networks, where we study and manipulate quantum states of matter and light with manifestly single quanta one-by-one. Moreover, the experimental realization of strongly correlated quantum systems of atoms and photons expands the frontiers of exquisite quantum control of entangled states with diverse applications from quantum information science, to atomic and condensed matter physics, to precision metrology, and to quantum biology. In relevance to quantum many-body physics [39,40], measurements, and controls [41], I would like to present two questions as important underlying motivations for my research, which I hope to make contact with in the remaining chapters.

1. Can quantum coherence and entanglement exist and be preserved in quantum many-body systems, either spontaneously acquired or externally induced by lasers?

2. How do we measure, manipulate, and utilize quantum entanglement in mesoscopic systems?

1.2 Ensemble-based quantum information processing and Duan-Lukin-Cirac-Zoller protocol

Historically, the investigation of collective interactions between atoms and photons began with the striking prediction[42] by Robert Dicke in 1954 that the radiative decay rate for an assembly of atoms in the excited state can be significantly modified. Under certain circumstances, the spontaneous emission of the excited state can be considerably enhanced by a 'phase-locking' of atomic dipoles with dynamic evolution of the atomic state confined within a class of symmetric collective spin states[43], a cooperative phenomena known as "superradiance" (see ref.[44] for an excellent review of theoretical descriptions of superradiant effects observed in different regimes; see also chapter 2). Since then, collective interactions have been observed in diverse systems, with a recent survey including the studies of dynamic phase transitions[45,46] and collective Lamb shifts[47], leading to the development of quantum interfaces for storing and retrieving quantum information in atomic ensembles[48].

Contemporary with these advances, various theoretical protocols have been developed for the realization of scalable quantum networks with atomic ensembles[49], including the seminal proposal by Luming Duan, Mikhail Lukin, Ignacio Cirac, and Peter Zoller (referred as the *DLCZ* protocol hereafter) in 2001 (ref.[4]). The introduction of the *DLCZ* protocol has led to a development of a remarkable worldwide community with significant achievements in the creation and distribution of entanglement. In this section, I will review recent progresses by other groups towards ensemble-based quantum memory to put the researches described in this thesis into context.

Generally, strong nonlinear interaction is required to generate nontrivial quantum resources for quantum information science. For ensemble-based quantum information processing, three important approaches to

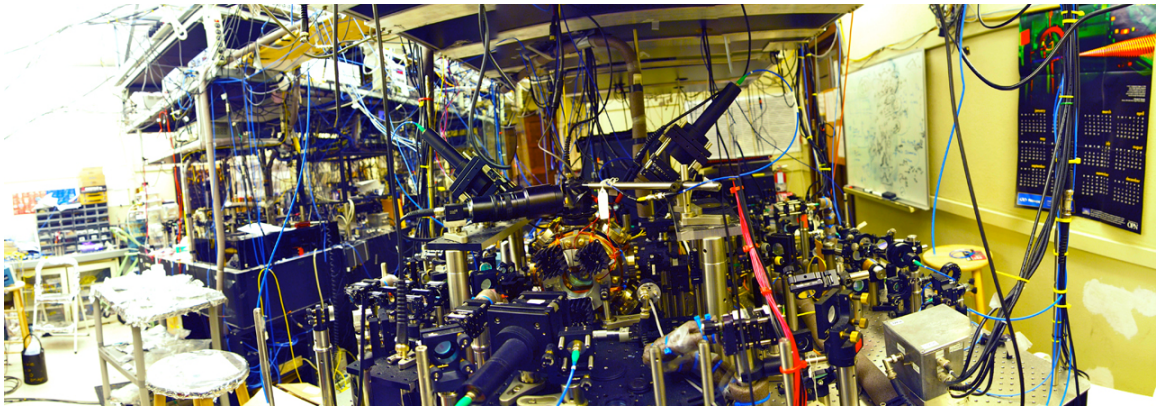

Figure 1.2: **A matter-light quantum interface in action for my experiments[30,33,34,36,37].** Cold ensembles of $\sim 10^{10}$ Cesium atoms are (i) laser cooled and trapped to $10-100$ μK, and (ii) prepared to specific ground states $|F, m_F\rangle$ via hyperfine and Zeeman pumping. In step (iii), we operate the quantum interface where the atomic quantum information (QI) is generated and stored in the ground state coherences for the hyperfine levels $|g\rangle = |F=4\rangle$, $|s\rangle = |F=3\rangle$ of the electronic ground state $6S_{1/2}$. Finally, (iv) we read out the atomic states to photonic states, and (vi) detect the photonic QI for quantum-state characterization.

matter-light interactions $\hat{H}_{\text{int}}$ have been developed for continuous and discrete quantum variables[48]. In the setting of continuous variables[48,50], major achievements have been made with quantum nondemolition interactions $\hat{H}_{\text{int}}^{(\text{QND})} \sim \chi_{\text{QND}} \hat{P}_\gamma \hat{P}_a$ between the transverse spin components for the collection of atoms a and polarizations of light γ based on the off-resonant Faraday rotation of a probe beam[51–58]. While the atomic state in this case is not directly optically accessible, it can also be mapped to an optical field by way of teleportation. Notable advances have been the entanglement of macroscopic spin states for two atomic ensembles[59], quantum teleportation from light to matter[60], multiparticle entanglement for atoms within an ensemble[61,62], and dissipation-induced entanglement via reservoir engineering[63]. In addition, quantum measurements have been actively pursued for quantum-enhanced atom interferometry via spin squeezing (see, e.g., refs.[64–69]). Despite the spectacular advances in this field[48,50], experiments in this thesis investigate the strong interaction of single photons and collective excitations in atomic ensembles in the limit of weak excitations $\xi \ll 1$, where $\simeq |\xi|^2$ is the mean number of collective excitations.

As pioneered by *DLCZ*[4], parametric Raman interactions, $\hat{H}_{\text{int}}^{(\text{par})} \sim \chi_p \hat{a}_\gamma \hat{S}_a + h.c.$, based on the weak $\chi^{(3)}$ nonlinearity of the system[70] can be applied for robust implementations of quantum communication protocols, including quantum cryptography and teleportation (chapter 2). In the regime of single excitations ($\xi \ll 1$), the required 'strong' nonlinearity is provided by projective measurements. An important aspect of this approach is that the heralded atomic state can be coherently mapped to single photons in an efficient manner via the collective matter-light interaction $\hat{H}_{\text{int}}^{(\text{map})} \sim \chi_m \hat{a}_\gamma \hat{S}_a^\dagger + h.c$ (chapter 2). In particular, parallel chains of heralded entangled states can be converted into polarization entangled photons via entanglement connection (ref.[37], chapter 5) and distribution (ref.[36], chapter 6), with a built-in purification mechanism[4]. For a preamble to the original protocol, I refer to James Chou's thesis[71] and ref.[49]. In chapter 2, I will revisit the interaction Hamiltonians $\hat{H}_{\text{int}}^{(\text{par})}$ and $\hat{H}_{\text{int}}^{(\text{map})}$, and derive the steady-state solutions for $\hat{H}_{\text{int}}^{(\text{par})}$ as well as the equation of motions for $\hat{H}_{\text{int}}^{(\text{map})}$ in detail. I refer to Fig. 1.2 for a standard routine of our experiments.

In 2003, initial experiments for the *DLCZ* protocol began with the observations of quantum correlations between photon pairs emitted from an ensemble by our group (ref.[72]; see also James' thesis[71]) and by the group of Mikhail Lukin[73]. Since then, single photons were generated in a heralded fashion by reading the stored, collective excitations to propagating fields[74–80]. Conditional efficiencies 74% in free space[81] and 90% in a cavity[82] were achieved for retrieving a single excitation in the ensemble to a single photon. Off-axial phase-matching configuration for the four-wave mixing process has been pioneered by Steve Harris' group[75] and used extensively in our experiments, whereby we generate spatially separate quantum fields from the classical beams. However, as I will discuss in chapter 2, the collective spin waves generated in this fashion can have considerably shorter coherence length l_c as well as a Doppler life times τ_d than the collinear configuration.

With these capabilities for collective emissions in hand, our group generated heralded entanglement between distant ensembles in 2005 (ref.[27]; see James' thesis[71] for this remarkable piece of work). Although the degree of entanglement was small in the initial experiment[27], more recently we have been able to infer the

concurrence $C = 0.9 \pm 0.3$ for the entanglement associated with density matrix of the two ensembles (ref.[34], chapter 3). Since then, substantial progresses have been made with heralded quantum states (section 3.7), including the synchronization of indistinguishable single-photon sources[78–80] and heralded storage of polarization qubits[83]. Furthermore, Vladan Vuletić's group demonstrated that two ensembles can be entangled via the adiabatic transfer of heralded excitations in a cavity[29].

The *DLCZ* protocol is based upon a quantum repeater architecture involving independent operations on parallel chains of entangled systems, with scalability relying critically upon the conditional control of entanglement. In 2007, we took an important step towards this goal by achieving the minimal functionality required for scalable quantum networks via the asynchronous preparation and control of heralded entanglement (ref.[36], chapter 4). In this experiment[36], we distributed a pair of heralded number-state entangled states and converted them to an effective polarization entangled state, thereby violating Clauser-Horne-Shimony-Holt (*CHSH*) inequality[84] (chapter 4). Using this setup, we also established quantum coherence between ensembles that never interacted in the past by way of entanglement connection (ref.[37], chapter 5). Later, Jian-Wei Pan's group also realized elementary quantum nodes for a Briegel-Dür-Cirac-Zoller (*BDCZ*) quantum repeater[9] in 2008 (ref.[85]).

In parallel with the research on *heralded* entanglement, there has also been considerable interest in the development of *deterministic* quantum interfaces to achieve reversible mapping of quantum states of light to and from atomic ensembles via $\hat{H}_{\rm int}^{(\rm map)}$ (refs.[86,87], chapter 2). Inspired by the early pioneering experiments on ultraslow-light propagation in dense atomic medium in 1999 (refs.[88,89]), storage and retrieval of optical pulses have been demonstrated, for both classical pulses[90,91] and single-photon pulses[92,93] by way of dynamic electromagnetically induced transparency (EIT) (refs.[86,94–96], chapter 2). Similarly, quadrature squeezed states have been stored and retrieved in an ensemble in 2008 (refs.[97,98]). In 2008, we achieved an important milestone for transferring quantum entanglement over quantum networks by demonstrating the *reversible* mapping of photonic entanglement to and from two quantum memories by the EIT process (ref.[30], chapter 6). In this experiment, we prepared an entangled state of light from an "offline" source ensemble, and mapped the photonic entanglement into and out of two atomic ensembles (chapter 6). Our work on reversible quantum interfaces thereby sets the stage towards integrating hybrid quantum systems by way of photonic quantum buses (chapter 10). Recently, this approach has been extended to transfer the initial atom-photon entanglement in a cavity QED system to an entangled state of a single atom and a Bose-Einstein condensate in 2011 (ref.[99]).

Since then, a wide variety of approaches has been proposed for storing and retrieving quantum states of light in inhomogeneously broadened samples, including controlled reversible inhomogeneous broadening (CRIB) (ref.[100]), atomic frequency comb (AFC) (ref.[101]), and gradient echo storage (refs.[102,103]); see also ref.[104] for a comprehensive review. Many of these storage techniques offer unique perspectives for high-bandwidth multimode quantum memories and integrated waveguide coupling, and several groups have reported important progresses towards this goal, such as electric control of photon echos[105], coherent pulse

sequencing in atomic vapor[106] and storage of temporal modes in rare-earth solid-state ensembles[107], albeit with classical states. A vast majority of these experiments, however, do not demonstrate a *genuine* quantum memory in that they use classical states detected by postselection, and rely on the "rephasing" of the collective emissions after a uncontrollable fixed delay. More recently, time-bin entangled states have been partially stored and retrieved after a predetermined delay in 2011 (refs.[108,109]). In these experiments, however, the entangled states were detected in a *post-dicted* fashion without the possibility of mapping the *physical* state of light onto the atomic ensembles[110] (section 3.7). Nevertheless, experiments listed here represent significant advances of multimode quantum memories towards "practical" quantum repeaters[49].

Other experiments not described here are those based upon entanglement as *post-diction*, for which the physical state is not available for subsequent utilization[110] (see section 3.7 for the multiple flavors of entanglement). For example, entanglement between two remote atomic ensembles has been generated in a *post-dicted* fashion[111], and *a posteriori* teleportation has been used to transport the polarization state of light to an atomic memory[112]. In addition, ref.[113] has claimed to have generated a particular kind of a multiphoton mode-entangled state, known as a *NOON* state, and applied for measuring the collective motion of the ensemble with phase super-resolution in a "spin-wave" interferometer, although the entanglement was not verified.

The figure of merits for the collective enhancement of matter-light interaction are high retrieval efficiency[81,82] and long memory times (chapter 2). 2009 was an intense year for the 'ensemble' community to increase the storage time for collective excitations in atomic ensembles leading to a worldwide effort, with the advances ranging from millisecond quantum memories[114,115], to light storage in an atomic Mott insulator[116], and finally to the longest memory time of "1.5 seconds" for storing a coherent state in a Bose-Einstein condensate[117]. However, in most of these experiments, the retrieval efficiencies were still $\eta \lesssim 1\%$. Important experiments preceding these activities have been the demonstration of the EIT storage of coherent states in a crystal with a storage time longer than 1 second (ref.[118]), the collapse and revival of collective excitations in an atomic ensemble[119,120], and the characterization of decoherence for the heralded entanglement stored in two atomic ensembles (ref.[34], chapter 3).

Around the same time, we began to collaborate with Pavel Logouvski and Steven van Enk to develop an *efficient* theoretical protocol for verifying multipartite mode-entangled W states (ref.[38], chapter 7). We proposed to use quantum uncertainty relations[121] as a nonlinear, nonlocal entanglement witness capable of verifying *genuine* W states, and of distinguishing the 'global' N-partite entangled states from any $(N-1)$-partite entangled states as well as their mixtures[38]. By implementing this verification protocol, we generated and characterized the multipartite entanglement for one photon shared among four optical modes in 2009 (ref.[35], chapter 8).

Finally, in 2010, we made a major advance towards multipartite quantum networks by achieving measurement induced entanglement of spin waves among four quantum memories (ref.[33], chapter 9). The individual atomic components for the entangled W state of the four ensembles were coherently mapped to four entan-

gled beams of light, where we observed the statistical and dynamic transitions for the multipartite entangled spin waves (see Fig. 1.2 for the photo of the lab at the time). We also showed that our entanglement verification method is suitable for studying the entanglement order of condensed-matter systems in thermal equilibrium[33]. With regard to quantum measurements, the multipartite entangled state stored in the quantum memories can be applied for sensing an atomic phase shift beyond the limit for any unentangled state[33].

The original *DLCZ* protocol[4] has by now motivated an active field of theoretical study of quantum repeater architectures for optimizing the network scalability in view of actual laboratory capabilities[49,122–125]. Specific attentions have been made to the scaling behavior for multimode quantum repeaters[49], dynamic programming search algorithms[124], and entanglement percolation[6]. Moreover, measurement-based quantum computation has been proposed for scalable quantum computing with atomic ensembles[126]. Stationary dark-state polaritons in a standing-wave EIT medium have been proposed for strong photon-photon nonlinear interactions and quantum gates[127–130]. Single-photon entanglement purification was proposed[131] and partially demonstrated[132], but the higher-order excitations for the purified states have not been characterized[110].

By and large, significant advances of solid-state ensembles (e.g., rare-earth crystals[104]) and the achievement of *collective* strong coupling in diverse systems[133–138] have also contributed indirectly to our research program towards ensemble-based quantum information processing with neutral atoms, as described above. Collective strong coupling has been observed with Bose-Einstein condensate[133,134] and with an ensemble of trapped ions forming a Coulomb crystal[135] in the optical domain, and electron spin ensembles residing in diamonds have been coupled to a superconducting cavity in the microwave domain[136,137]. In addition, temporal modes of microwave photons have been stored and retrieved in an electron spin ensembles using a gradient echo technique[138]. Beyond the free-space experiments in this thesis, such advances are relevant to the outlook of our project (chapter 10), whereby we hope to investigate the strong interaction of heterogeneous quantum systems of atoms, photons, and phonons by way of photonic crystal nanowires[139] and atomic ensembles[a], and to distribute quantum coherence and entanglement over 'lithographically patterned' quantum networks.

1.3 My history in the group, and notable omitted results

Substantial progresses have been made in lab 2 including the heralded entanglement between two remote atomic ensembles[27], as noted above. As a result, upon my arrival in 2006, many parts of the apparatus in lab 2 were built by my predecessors, James Chou, Hugues de Riedmatten, Daniel Felinto, Alex Kuzmich, Julien Laurat, and Sergey Polyakov, since their initial work in 2003.

I acquired significant feedback and "lab lore" from James and Julien during my short overlap with them (2006–2007); see Kevin Birnbaum's thesis[142] for the definition of the term, "lab lores." I would thus like to acknowledge the early works in James' thesis[71], which formed an important basis to my experiments after 2006. Also, my training in atomic physics in Hal Metcalf's group (Stony Brook University) helped

[a] See also refs. [140,141] for new regimes of strong coupling, which may be achieved in the new system.

me to complete many tasks in this thesis in a timely fashion, including the coherent control of populations in Rydberg atomic beams by way of electromagnetically induced transparency (EIT) and stimulated Raman adiabatic passage (STIRAP).

Since 2006, we have made significant changes to the setup from experiment to experiment, and I will not be able to list the specific changes in this thesis. The details are documented throughout my lab notes, as well as those of my colleagues (James Chou, Hui Deng, Akihisa Goban, Julien Laurat, and Scott Papp). But some changes are noted in chapter 9. At the same time, I have tried, as others have in the past, to transfer as many "lab lores" and new techniques as possible to other members in lab 2.

As listed in the previous section, I have been involved in a number of experiments (chapters 3–10 in the thesis) since 2006. However, I regret that there are some results that I must omit in order to focus on experimental and theoretical results under the encompassing theme of quantum networks. I would thus like to take this opportunity to compile notable results not discussed in this thesis, to which my colleagues and I have contributed.

1.3.1 Coherent Rayleigh scattering

In 2007, I theoretically considered the possibility of using elastic Rayleigh scattering to measure the relative phase ϕ (ref.[145]) between two entangled ensembles to directly confirm the presence of the purported 'number-state' entanglement $\frac{1}{\sqrt{2}}\left(|\overline{g}_L\overline{s}_R\rangle + e^{i\phi}|\overline{s}_L\overline{g}_R\rangle\right)$ between the two ensembles in the 'cryptography' experiment (ref.[36], chapter 4). In this experiment[36], ϕ was fluctuating over the time scale of the experiment but was stable over the memory time $\tau \approx 10\ \mu s$. Because of the non-collinear geometry for the paths of the classical writing and reading pulses, and that of the non-classical fields 1 and 2, it was impossible to lock the interferometric paths to stabilize the relative phase ϕ. Nonetheless, I emphasize that the experiment[36]

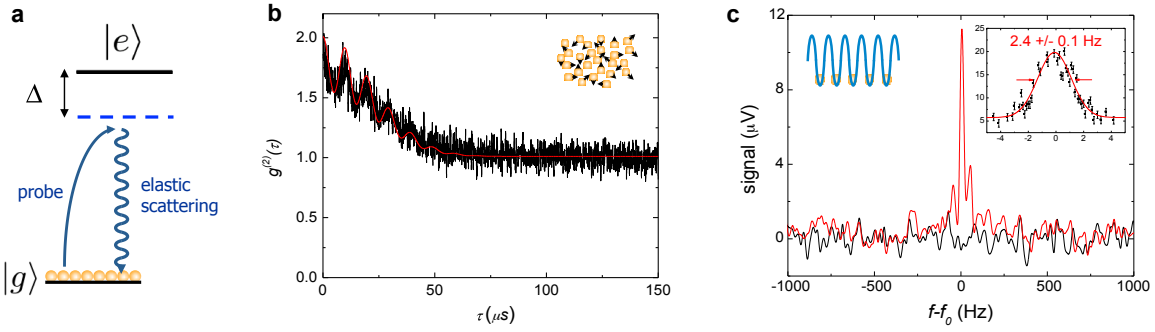

Figure 1.3: **Elastic Rayleigh scattering from atomic ensemble.** **a**, A red-detuned probe laser illuminates a cold sample of Cesium, generating elastically scattered photons[143–145]. **b**, The time-domain measurement of the photon counting statistics $g^{(2)}(\tau)$. The red solid line is a numerically simulated steady-state solution of $g^{(2)}(\tau)$, given the measured Zeeman splittings, the orientation of the magnetic field, and the temperature of the thermal atoms. **c**, Frequency-domain measurement of the linewidth of the scattered photons in the presence (absence) of atoms, as shown by the red (black) curves. The inset shows a high-resolution spectrum of the elastically scattered photons, revealing *Lamb-Dicke* narrowing.

unambiguously verified the entanglement, as we have observed polarization entanglement via the violation of *CHSH* inequality between two quantum nodes, for which we *locally* converted a pair of the purported number-state entanglement into polarization entanglement (ideally with $1/2$ of ebits).

In 2009, Scott and I made a partial measurement to show that the phases among the quadripartite entangled atomic ensembles (chapter 9) can be probed in principle (Fig. 1.3). We applied a red-detuned probe laser (detuning $\Delta = 10$ MHz from the cycling transition between ground state $|F = 4, m_F\rangle$ of $6S_{1/2}$ and excited state $|F = 5, m_F\rangle$ of $6P_{3/2}$) on an atomic sample with saturation parameter $s \ll 1$, such that the scattering process is dominantly elastic[143–145]. The time-domain measurement (Fig. 1.3b) of the photon counting statistics $g^{(2)}(\tau) \simeq 1 + |g_0^{(1)}(\tau)|^2$ (thermal atoms at $T_d \simeq 150$ μK without trapping) and the frequency-domain measurement (Fig. 1.3c) of the linewidth of the scattered photons from the trapped atoms revealed both the motional dephasing of the atoms and potentially the relative phase between the local oscillator and the scattered photons. The presence of residual magnetic field along the $\vec{k}$-vector of the probe beam induced an additional modulation on $g^{(2)}(\tau)$ for the Rayleigh scattered photons (Fig. 1.3b), due to the interferences of distinct (m_F) pathways for the $|F = 4, m_F\rangle \leftrightarrow |F = 5, m_F\rangle$ transition. The motional states of the atoms were simultaneously cooled and confined by the polarization gradient mechanism in Fig. 1.3c, thereby suppressing the motional dephasing rate down to 2.4 ± 0.1 Hz (limited by the mechanical instabilities in the measurement process). This allowed us to perform a recoil-free spectroscopy via elastic Rayleigh scattering in Fig. 1.3c (thanks to the *Lamb-Dicke* narrowing for the trapped atoms[146]).

1.3.2 Motional dephasing of spin waves

I analyzed theoretically the motional dephasing of spin waves given our phase-matching configuration, after observing an unexpected Gaussian decay of the retrieval efficiency in 2007 (see the result of ref.[34], chapter 3). Formerly, we have considered the motional dephasing only for atoms leaving the excitation region[147]. However, it turns out that the much smaller 'coherence length' for the 'timed' Dicke states[148] depends critically on the phase-matching configuration for the coherent radiation to take place, given the spatial phases encoded on the atoms (chapter 2). Independently, such a possibility was considered in the experiments by Vladan Vuletić's group[82], where they observed two time-scales for the memory time associated with the forward (long-lived) and backward (short-lived) propagating spin waves. Unfortunately, we did not pursue this idea in our experiments to improve the storage time beyond 1 ms (chapter 2).

Later, the groups of Alex Kuzmich and Jian-Wei Pan achieved millisecond quantum memories in 2008 by confining the spatial motion of the atoms[115] and by increasing the coherence length of the spin waves[114], respectively, which confirmed the validity of this idea. In our lab, the Rayleigh scattering measurements in 2009 agreed with the prediction of motional dephasing, whereby we cooled the motional state of the atoms in a near-resonant lattice formed in the process of polarization-gradient cooling[144], and inferred a motional dephasing rate $R_d = 2.4 \pm 0.1$ Hz (Fig. 1.3). In addition, we have reduced the net momentum transfer $\delta\vec{k}$ (i.e., increasing the coherence length) of the spin waves to achieve coherence times $\tau_m \simeq 60$ μs, limited at

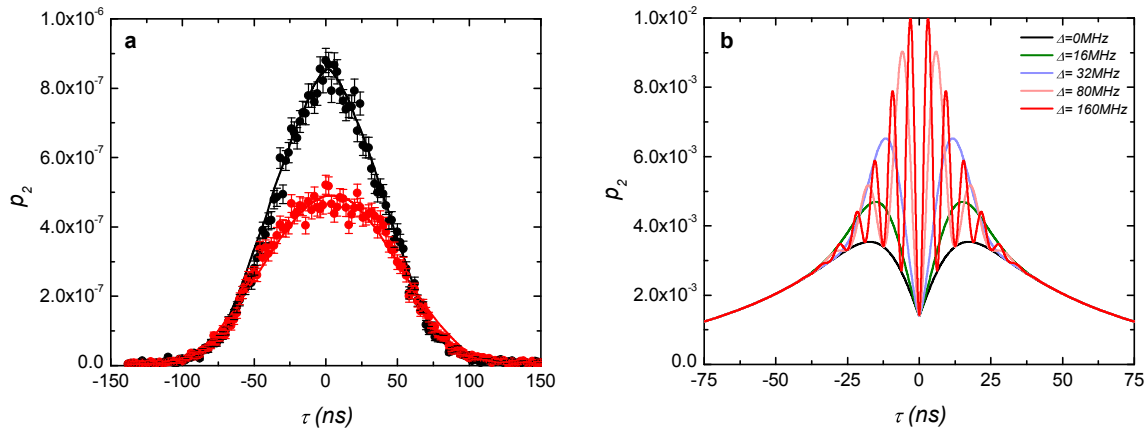

Figure 1.4: **Towards quantum interference between indistinguishable single photons emitted from an atomic ensemble and a single atom in a cavity. a**, Time-resolved Hong-Ou-Mandel (HOM) interference [149] between two coherent states. As a control experiment, we interfere two balanced coherent states emanated from each lab with orthogonal (black) and parallel (red) polarizations, where the temporal profiles of the pulses are matched close to the emission patterns of the single-photon sources. We achieve HOM visibility $V_{\mathrm{HOM}}(\tau = 0) = 0.52 \pm 0.08$ at delay $\tau = 0$ ns, similar to our expectation $V_{\mathrm{HOM}}^{\mathrm{theory}} = 0.5$ for balanced coherent states. The theoretical model (line) is based on the numerical procedure described in ref. [150], using the measured spatio-temporal modes for each beam. **b**, Simulation of the quantum interference between two indistinguishable single-photons with the ensemble cross-correlation function set at $g_{12} = 50$. We theoretically calculate the time-resolved HOM interference for various detuning Δ between the two photons, given the temporal profiles of the two transform-limited single-photon sources.

the time by the inhomogeneous Zeeman broadening in late 2007 (chapter 2, see Fig. 2.8). While these may be considered as missed opportunities, I believe that we followed the 'right' footsteps (chapters 7–9) in order to pursue more interesting ideas for my doctoral thesis.

1.3.3 Indistinguishability between heterogeneous single-photon sources

In mid-2007, we began to collaborate with the cavity QED lab (Andreea Boca, Dave Boozer, Russell Miller and Tracy Northrup in lab 11) to study the time-resolved Hong-Ou-Mandel (HOM) interference [149] between two indistinguishable single photons emitted from an ensemble and a single atom in a cavity. While we have not been able to succeed in this experiment with sufficiently large suppression for the two-fold coincidence between the two output ports of the interferometer, there were discussions regarding the non-classicality of HOM interference. During this time, I also analyzed experimentally and theoretically the temporal profile of the HOM interference for two photons emanating from each lab (see, e.g., Fig. 1.4).

1.3.4 Inducing phase shifts between collective excitations stored in atomic ensembles for quantum-enhanced phase estimation

In early 2010, Aki, Lucile, and I explored the possibility of randomly inducing a π phase shift on one of four atomic ensembles, following Steven's idea to employ a quantum-enhanced parameter estimation protocol

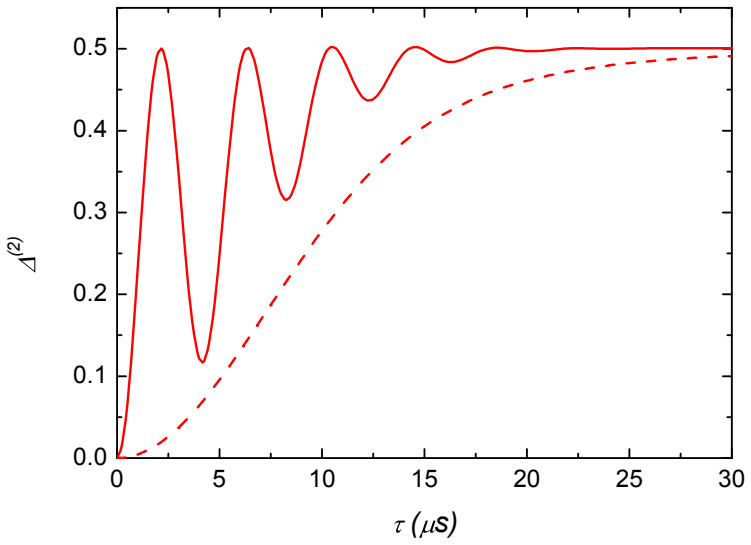

Figure 1.5: **A phase shift in the collective excitation due to an off-resonant ac-Stark shift beam.** Theoretically simulated variance $\Delta^{(2)}$ for two ensembles as a function of storage time τ, including inhomogeneous broadening from the ac-Stark shift beam. A dashed line shows the result of $\Delta^{(2)}$ without a light- shift beam, whereby $\Delta^{(2)}$ increases due to motional dephasing. We define $\Delta^{(2)} = 1 - p_{10}^2 - p_{01}^2$, where p_{10} and p_{01} are the normalized output probabilities after interfering two entangled fields (chapters 8–9).

(partially discussed in ref.[33] and chapter 9). The idea was to induce a phase shift on the ground state coherence $|F = 3\rangle - |F = 4\rangle$ by switching on an off-resonant beam. This phase-shift beam would interact with the collective excitations $|\overline{s}\rangle_k$ in a direction not phase-matched to $|\overline{s}\rangle_k$, thereby avoiding any possible collective enhancement of accidentally erasing the spin waves. In the process of this study, Lucile worked with Aki to intensity stabilize the ac-Stark shift beam I_{ac} and to lock an interference filter laser[151] to a fiber Fabry-Perot reference cavity. Aki developed a simple model for simulating the phase shifts and scattering rate for a given power I_{ac}, as shown by Fig. 1.5. However, according to our estimates, the required retrieval efficiency and the quantum efficiency to observe any quantum enhanced sensitivity (overall efficiencies of $\simeq 75\%$ for unambiguous state-discrimination protocol and $\simeq 93\%$ for minimum error discrimination protocol) proved difficult (if not impossible) with our current experimental capability.

1.3.5 Technical side-projects

1.3.5.1 Development of double-sided AR-coated UHV glass cell

In the early days, Julien and I had worked with Ron Bihler, then at Technical Glass, Inc., to prototype a ultra-high-vacuum (UHV) glass cell with double-sided anti-reflection (AR) coating on the windows. Although I will not discuss this side-project in the thesis[b], the new "frit-fusing" technique, which Ron developed in

[b]Initially, Julien and I worked with Ron Bihler (Technical Glass, Inc., now at Precision Glassblowing, Inc.) to use vacuum compatible glass epoxies (e.g., Epotek 353ND) and Vacseal to seal AR-coated cells, but it proved to be very fragile during bakes in 2006. Later, I worked with Kazuyuki Tsukamoto (Japan Cell) and Ron in 2007 to create a robust AR-coated UHV Pyrex cell by optically contacting polished glasses assisted with local heating of standard glass frits. Ron later extended this approach to develop his low-temperature frit-fusing method.

2007, combines the traditional optical contacting method with special low-temperature frits, and allows for fusion-bonding optical quality fused silica/quartz windows without damaging the AR coating. While I have considered using this cell for the next generation vacuum chamber at the time, unfortunately we have not pursued this project further because of some fear of developing fractures in the frits over time. However, I would like to note that several groups in JILA, Paris, and Stanford have by now used these cells in their BEC experiments successfully, where they have maintained pressures under 10^{-10} Torr over the last couple of years. It may be interesting to revisit this idea in the future.

1.3.5.2 Filtering quantum fields at the single-photon level from the strong classical beams

In 2008, Hui and I characterized a photo-refractive fiber Bragg grating from AOS, which Russ and Tracy have investigated before. Despite the narrow bandwidth ($\nu = 500$ MHz), the transmission was not superior to our existing setup using the Cs filter cells with paraffin coating (attached with AR-coated windows). Scott has also looked into a custom fiber cavity (Micron Optics), where the transmission was inferior to the fiber Bragg grating. I have looked into custom fiber wavelength division multiplexers (WDM) and circulators from Canadian Instruments and Research Limited (CIRL) and Oz Optics at 852 nm, which was later found to be unfavorable due to transmission loss and Brillioun scattering noise from the locking lasers in a test at CIRL. Later, Daniel in lab 1 carried on with studying the WDMs for the fiber trap in 2010.

In 2009, Aki and I characterized a custom AR-coated frit-fused Cs vapor cell with paraffin and buffer gas (Technical Glass, Inc., now part of Precision Glassblowing of Colorado) hoping for a better optical quality with the help of double-sided AR coating (section 1.3.5.1). However, the thermally redistributed paraffin contaminated the polished windows and subsequently limited the transmission as well as the wavefront distortion.

A recent reincarnation of this project has been made with my work in late 2010 with Dr. Vadim Smirnov and Dr. Igor Ciapurin at OptiGrate to produce a custom holographic grating (VBG) (Fig. 1.6a) from a photo-thermo-refractive (PTR) glass that provides an unprecedented filtering capability for the quantum fields to avoid contamination from the classical trapping beams for the fiber trap by ~ 180 dB extinction ratio and $> 95\%$ diffraction efficiency (chapter 10). Our test on the VBGs agrees well to the simulation based on coupled mode theory[152] (Fig. 1.6b). Formerly, such an attempt has been made successfully in Allan Migdall's group at NIST.

1.3.5.3 Other projects

There have been other side-projects contributing to the group in general, which I will not discuss here in detail, as Scott's work on generating pulse trains and logic gates with field programmable gating arrays (FPGA) (National Instruments) for atomic ensemble experiments[c]. While Scott and I determined that the FPGA's timing noise was insufficient for our experiments (chapters 8–9), lab 1 later used this FPGA for their

[c]Formerly, James Chou tested slower Spartan FPGAs from Xilinx.

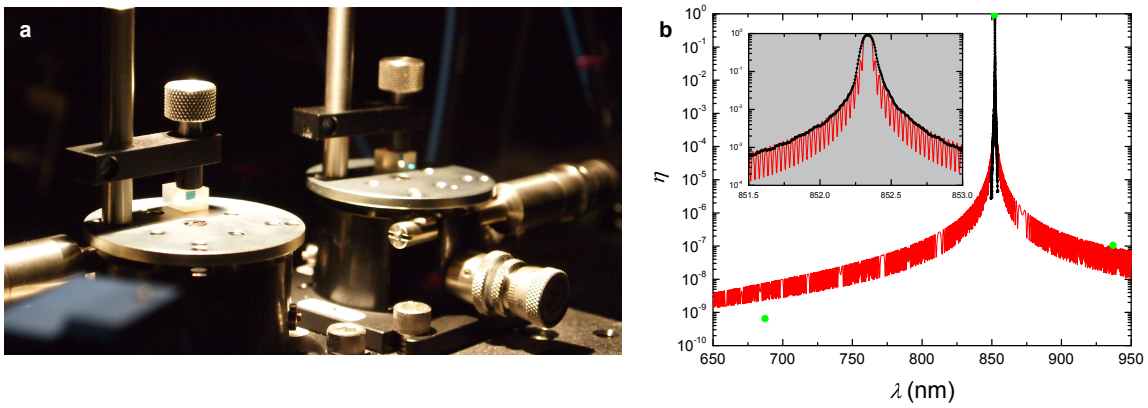

Figure 1.6: **A custom made high-performance PTR-based volume Bragg grating.** **a**, Volume Bragg grating (OptiGrate, Inc.) mounted on a high-precision 3-axis tilt-roll mount ($\sim \mu$rad sensitivity). **b**, Spectral dependence for a single volume Bragg grating. The measured extinction ratios *ER* (green circle) for the red-detuned and blue-detuned trapping beams at $\lambda = 687$ nm and 935 nm are 70 and 92 dB, respectively. The black circles are the measured diffraction efficiency around resonance. The diffraction efficiency on resonance ($\lambda_0 = 852.35$ nm) is $\eta_{\rm DE} = 93.5 \pm 0.3\%$, limited by the broadband AR coating. The red curve is a simulation based on coupled mode theory [152]. The spectral bandwidth (FWHM) is designed to be $\delta\nu = 30$ GHz and the intrinsic diffraction efficiency is $\eta_{\rm DE}^{\rm (int)} = 99.9\%$, according to my calculations for a Gaussian beam of $w_0 \simeq 1$ mm.

experiment [153]. In chapter 9, we implemented an alternative solution by way of a quantum composer and digital logic gates.

Aki and I also updated the diode laser's circuitries as well as other electronics[d]. Scott and I designed various electronic servos for locking interferometers and standard Fabry-Perot cavities, as well as for intensity stabilizations, and various logic circuits for pulse triggers, controls, and synchronizations. In appendix A, I list a few examples of the electronic circuit designs.

I characterized a variety of methods to image patches of atoms in a single collective excitation via microlens arrays ($w_0 \simeq 2$ μm with 80% filling factor) (SUSS MicroOptics and Jenoptik) and lensed fiber arrays ($w_0 \simeq 600$ nm with 5% filling factor) (Seikoh-Giken). Scott characterized ball lenses (Laseoptics) and tapered lens fibers (Nanonics) for imaging single atoms[e] ($w_0 \simeq 400$ nm). More detail on these and other projects can be found in our lab notes and written notes, and in the "lab 2 disc," which compiles all the electronic files for the printed circuit boards (PCB) in lab 2 since 2006.

1.4 List of recent advances

To summarize the advances made in this thesis, I hereby list major achievements that my colleagues and I have made over the last few years:

[d] See some examples in the 'blue book' of the electronics room and in the lab 2 disc (e.g., VCO designs, phase-sensitive detectors, high-bandwidth HV amplifiers, and piezo controllers).

[e] Later, the tapered lens fiber from Nanonics was used in lab 11a for trapping single atoms. Daniel Chao, Scott Kelber, Scott Papp, and Cindy Regal further characterized the fiber in detail.

1. Characterization of the dissipative process for heralded entanglement stored in atomic ensembles (chapter 3).

2. Realization of functional quantum nodes for entanglement distribution over a scalable quantum network (chapter 4).

3. Reversible mapping of photonic entanglement into and out of a quantum memory (chapter 6).

4. Characterization of entanglement for one photon shared among four optical modes via quantum uncertainty relations (chapter 8).

5. Coherent control of generation, storage, and transfer of multipartite entangled spin-waves to photonic multipartite entangled states (chapter 9).

In the remaining chapters, I will describe specific experimental and theoretical results of our work to substantiate the advances listed here, as well as others.